Journal of Computational Physics **150,** 239–267 (1999)
Article ID jcph.1998.6178, available online at http://www.idealibrary.com on IDEAL®

A Particular Solution Trefftz Method for Non-linear Poisson Problems in Heat and Mass Transfer

Karthik Balakrishnan* and Palghat A. Ramachandran†

Department of Chemical Engineering, Washington University, Saint Louis, Missouri
E-mail: *kb3@cec.wustl.edu and †rama@wuche3.wustl.edu

Received June 18, 1998; revised November 17, 1998

This paper proposes a computational procedure based on the Trefftz method for the solution of non-linear Poisson problems. The problem is solved by finding an approximate particular solution to the Poisson equation and using boundary collocation to solve the resulting Laplace equation. This method results in a global collocation and hence eliminates the need for discretization of the domain in both two and three dimensions. The solution procedure proposed earlier in the literature based upon the above method has been reformulated for increased computational efficiency. A quasi-Newton iteration method along with a new heuristic for source point location is used for efficient convergence of the numerical scheme. The efficacy of the new formulation has been demonstrated for two classes of problems, viz. the thermal explosion problem and the diffusion–reaction problem in a partially wetted catalyst pellet. A brief error analysis of the method, as well as future research directions, is presented. © 1999 Academic Press

Key Words: method of fundamental solutions; Trefftz method; approximate particular solution; non-linear Poisson problem; radial basis functions; matrix of particular solutions.

1. INTRODUCTION

Non-linear Poisson equations of the type $\nabla^2 u = f(x, u)$, where x is the position and u the dependent variable, are encountered in numerous problems in heat conduction, mass transfer, and flow through porous media. The solution to such problems is usually required in non-regular two- and three-dimensional geometries with non-uniform boundary conditions. The use of conventional numerical procedures, viz. finite differences, finite elements, etc., to solve these problems necessitates high levels of discretization, resulting in large computer time. Hence in recent years, there has been considerable interest to develop "mesh-free"

0021-9991/99 $30.00
Copyright © 1999 by Academic Press
All rights of reproduction in any form reserved.

methods, which do not involve extensive discretization of the domain of interest. Most common among such methods is the dual reciprocity boundary element method (DRBEM) [1, 2]. In this method, the weighted residual formulation of the governing differential equation is reduced to a set of line/surface integrals over the boundary in two and three dimensions, respectively, using the Green–Gauss identity. The method is closely related to the boundary integral method and differs only in the fact that in DRBEM, one transfers non-homogenous terms involved to equivalent boundary terms.

One of the drawbacks of boundary integral methods (and DRBEM) is that the formulation involves the evaluation of singular or near-singular integrals [3, 4]. The accurate evaluation of these singular/near-singular integrals can be computationally expensive due to the large numbers of quadrature points required in the vicinity of the singularity. This is compounded by the fact that large numbers of boundary nodes are necessary if lower order polynomial approximations are used for interpolation. One has to then trade off between the accuracy of the solution and the computational time especially for irregular geometries. On the one hand, inappropriate choice of discretization can lead to large errors in the solution, and on the other, a large amount of discretization causes slow convergence of the solution, especially for non-linear problems [1, 4].

To circumvent the problem of having to evaluate singular integrals, a class of boundary collocation methods classified under the generic name "Trefftz method" [5] can be used. Here the solution is represented using layer potentials on non-physical surfaces, thereby circumventing the need to evaluate any singular integrals. By adopting such a method, one also avoids the problem of complicated surface meshing required for the traditional BEM in three dimensions. In the Trefftz method, the solution is expanded in terms of basis functions satisfying the internal region exactly, and the boundary conditions are satisfied by collocation on the boundary only. Depending upon the kind of basis functions employed, one can classify it as either the T-Trefftz or the F-Trefftz method. Prior research on the implementation of the Trefftz method has focused mainly on the Laplace and biharmonic equations [6–16]. These studies have demonstrated the efficacy of the Trefftz method for the solution of the Laplace and biharmonic equations. These partial differential equations are linear and involve no non-homogenous terms. For the Poisson equation, however, a modification of the solution procedure is needed. To handle the Poisson terms, the problem is split into two parts, a homogenous part satisfying the Laplace equation and a particular solution, which is approximated over the domain. Thus a combination of the particular solution method with the Trefftz method, called the "Particular solution Trefftz method," offers the possibility of a computational technique which involves neither domain nor boundary discretization. Such a method would offer considerable computational advantage, especially for three-dimensional problems in non-regular geometries. The solution of the Poisson-type equations using this method has recently been studied by Chen and Golberg *et al*. [17–20]. The method was tested on specific forms of the forcing function (non-homogenous term) f, viz. (i) f is a function of position only and (ii) the Frank–Kamenettski equation for explosion and quenching problems, with promising results. However, the studies were restricted to regular geometries, with only Dirichlet boundary conditions being imposed, and no extensive parametric studies were reported. One therefore needs to investigate the method in detail for more complex problems in non-regular geometries with mixed boundary conditions. Furthermore, for the method to be viable as an alternative computational tool, the development of efficient convergence schemes is warranted. The primary goal of this paper is to present a new computational formulation of the Trefftz method for non-linear Poisson

problems, with improved convergence properties compared to a prior implementation of the method. The method's efficacy is demonstrated for a number of mixed boundary value problems.

The layout of the paper is as follows. In Section 2.1, we review the classical T- and F-Trefftz methods for the Laplace and linear Poisson problems. In Sections 2.2 and 2.3, we present the particular solution Trefftz method along with a prior implementation of the method. In Sections 2.4–2.6, we present the solution methodology adopted by us and its advantages, followed by a new heuristic criterion for location of source points in the scheme described in Section 2.8. Some illustrative examples are presented in Section 3, and an error analysis of the method is given in Section 4. In Sections 5 and 6, the findings are critically evaluated along with the scope for improvements and future work.

2. THE TREFFTZ METHOD FOR THE POISSON EQUATION

Consider the Poisson equation to be solved over a domain Ω in R^2 or R^3 with enclosing boundary Γ,

$$\nabla^2 u = f(\bar{x}, u) \qquad \text{in } \Omega, \tag{1}$$

where $\bar{x}$ represents the coordinates of the point

$$\bar{x} = (x, y) \qquad \text{in } R^2$$

$$\bar{x} = (x, y, z) \qquad \text{in } R^3,$$

with mixed boundary conditions,

$$\text{Dirichlet: } u = \bar{u} \qquad \text{over } \Gamma_1 \tag{2a}$$

$$\text{Neumann: } \frac{\partial u}{\partial n} = p = \bar{p} \qquad \text{over } \Gamma_2, \tag{2b}$$

where $\Gamma_1 + \Gamma_2 = \Gamma$.

The solution difficulty in using boundary methods arises due to the presence of a non-homogenous term f in Eq. (1). However, by finding an approximate particular solution, the problem can be reduced to the solution of the Laplace equation. This is elaborated upon in Section 2.2. We now briefly review the Trefftz method for the Laplace equation.

2.1. *The Classical Trefftz Method for Laplace and Linear Poisson Problems*

When the forcing function $f = 0$, Eq. (1) reduces to the Laplace equation, and when $f = \pm\lambda^2 u$, one has a linear Poisson problem (diffusion–reaction/Helmholtz equation, respectively). For such problems, the solution in the interior can be represented exactly by means of T-complete functions or the fundamental solution to the differential operator [8, 10, 11, 18]. The method is called T- or F-Trefftz depending on whether one uses the T-complete functions or the fundamental solution to the operator, respectively [5, 21]. In order to illustrate the procedure consider the Laplace equation,

$$\nabla^2 v = 0,$$

where the dependent variable is now changed to v for convenience of notation in later sections.

The solution can be expressed as

$$v = a_0 + \sum_{i=1}^{n} a_i G_i, \tag{3}$$

where the functions G_i for the F-Trefftz method are the solutions to

$$\nabla^2 G_i = -\delta(r_i) \qquad i = 1, n \tag{4}$$

and are given by

$$G_i = -\ln(r_i) \qquad i = 1, n. \tag{5}$$

The distance r_i denotes the distance between the ith hypothetical source point of unit strength and any arbitrary field point on the boundary or the interior of the domain. The functions G_i are made non-singular throughout the interior of the domain by locating the source points outside the domain of consideration. The F-Trefftz method is also referred to as the method of fundamental solutions [4, 22], charge simulation method [23], or singularity method [24]. For the T-Trefftz method, the functions G_i are called T-complete functions and the analytical expressions are given in Refs. [7, 13, 21].

Since the solution in the interior is satisfied exactly by v, one now needs to determine the parameters a_0 through a_n so as to satisfy the imposed boundary conditions. These unknown parameters a_0 through a_n can be evaluated by two methods, viz. collocation and Galerkin methods, as outlined below.

Collocation. Since the layer potential on the boundary is only an approximation to the exact solution, the difference between the two, the boundary residual R is given by

$$R_1 = v - \bar{v} \neq 0 \qquad \text{on } \Gamma_1$$
$$R_2 = p - \bar{p} \neq 0 \qquad \text{on } \Gamma_2.$$

In the collocation formulation, one chooses $n+1$ collocation points on the domain boundary and the residual of the error is set to zero, i.e., $R_1 = R_2 = 0$, at each collocation point. When the number of unknown parameters a_i $(i = 0, 1, \ldots, n)$ equals the number of collocation points, one has a set of $n+1$ linear equations for a Dirichlet problem. When the number of collocation points exceeds the number of unknowns, one uses the least square method to minimize the sum of the boundary errors.

Galerkin method. In the Galerkin method the weighted residual is forced to zero with the weighting function chosen to be same as the functions G_i. Thus one obtains

$$\int_{\Gamma_1} G_i(v - \bar{v}) + \int_{\Gamma_2} G_i\left(\frac{\partial v}{\partial n} - \bar{p}\right) = 0.$$

We restrict ourselves to the collocation formulation in this paper. Thus, the method leads to a grid-free solution scheme, with the only limitation that the optimal location of source points is unknown a priori, the details of which will be elaborated upon later.

2.2. *The Particular Solution Trefftz Method for Non-linear Poisson Problems*

For a non-linear Poisson problem, the T-complete functions (T-Trefftz)/fundamental solution (F-Trefftz) cannot be found analytically for a general case. Hence, one resorts to the method of particular solutions, similar to the one frequently used to solve ordinary differential equation in one dimension. In this paper, we restrict ourselves to the analysis of the F-Trefftz method along with the particular solution method.

Here the solution u to the differential equation is split up into a homogenous part v and a particular solution w, such that

$$u = v + w. \tag{6}$$

The particular solution w satisfies the equation

$$\nabla^2 w = f \qquad \text{in } \Omega \tag{7}$$

but need not satisfy any set of boundary conditions. The problem now is to find the particular solution w. The exact particular solution to the problem can be found only for a limited number of cases. In general, one has to find an approximate particular solution to the problem [25]. One method for obtaining the approximate particular solution is by quasi-Monte Carlo integration [19]. This method is rather cumbersome, and evaluation of the approximate particular solution requires a large number of quasi-random points to be generated. A more direct method is to interpolate the forcing function f using a set of basis functions over the domain. Now f is expressed as

$$f = \sum_{k=1}^{nt} \phi_k \alpha_k, \tag{8}$$

where nt is the number of interpolation points, ϕ_k represents the basis functions used for interpolation, and α_k's are the set of interpolating coefficients. Any set of basis functions can be used for interpolation, but radial basis functions have been found to be most suitable [26]. The use of radial basis functions to approximate the forcing function f is discussed in Section 2.5. The particular solution w for the problem is then found by integrating the equation

$$\nabla^2 w = \sum_{k=1}^{nt} \phi_k \alpha_k. \tag{9}$$

If now one defines a set of functions ψ_k satisfying

$$\nabla^2 \psi_k = \phi_k, \tag{10}$$

then the approximate particular solution is given by

$$w = \sum_{k=1}^{nt} \psi_k \alpha_k. \tag{11}$$

Explicit formulae for ψ_k can be found in many cases, corresponding to specific forms of ϕ_k, and these are presented in Section 2.5.

Having found the approximate particular solution one now proceeds to solve the v problem using the classical Trefftz method. The homogenous part v now satisfies the Laplace equation,

$$\nabla^2 v = 0 \qquad \text{in } \Omega, \tag{12}$$

with a modified set of boundary conditions,

$$\begin{aligned} v &= \bar{u} - w \qquad \text{over } \Gamma_1 \\ \frac{\partial v}{\partial n} &= \bar{p} - \frac{\partial w}{\partial n} \qquad \text{over } \Gamma_2. \end{aligned} \tag{13}$$

As outlined in Section 2.1, v is expressed as a linear combination of functions G_i, Eq. (3), which satisfy the Laplace equation exactly in the interior of the domain. The boundary conditions are now specified for the v problem as in Eq. (13).

The composite solution can now be represented as

$$u = v + w = a_0 + \sum_{i=1}^{n} a_i G_i + \sum_{k=1}^{nt} \psi_k \alpha_k. \tag{14}$$

The unknowns are the parameters a_0 through a_n and the values of α_k (for $k = 1, nt$). The α_k's are in turn related to the values of f at the interpolation points. Thus, when f is a function of u, the unknowns are the a_i's ($i = 0, 1, \ldots, n$) and the values of u at the interpolation points. An illustrative location of the collocation points and the source points for a simply connected domain is given in Fig. 1.

2.3. *Numerical Implementation: Some Prior Attempts*

We now discuss the numerical implementation of the collocation scheme described in the previous section. This is necessary to put our solution methodology in proper perspective. To evaluate the particular solution, one needs to determine the interpolating coefficients α_k.

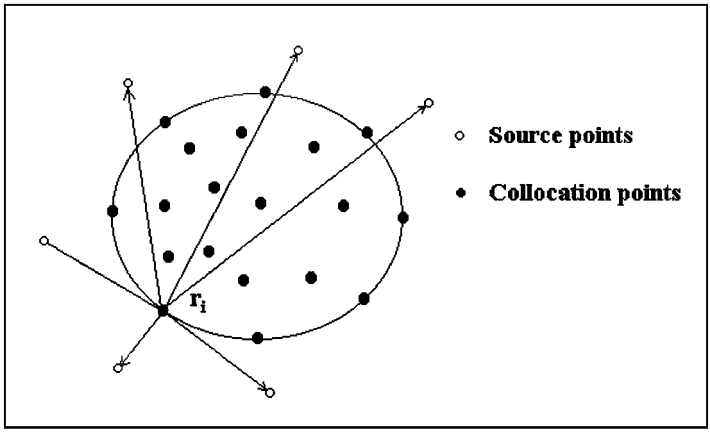

FIG. 1. Collocation points and source points for the F-Trefftz method.

To do so one applies the interpolation condition at all the collocation points, viz.

$$f_j = \sum_{k=1}^{nt} \phi_{jk}\alpha_k \qquad j = 1, 2, \ldots, nt, \tag{15}$$

where ϕ_{jk}'s are the interpolating functions evaluated at the jth point.

Alternatively,

$$\boldsymbol{\alpha} = \Phi^{-1}\mathbf{f}, \tag{16}$$

where $\boldsymbol{\alpha}$ is the vector of coefficients comprising α_k's, Φ^{-1} is the inverse of matrix of ϕ_{jk}'s, and $\mathbf{f}$ is the vector of f values at interpolating points. Thus the α_k's can be determined by solving a set of nt linear equations.

When f is a function of only the spatial variables, the values of f at the collocation points are known a priori. The calculation of the coefficients α_k does not involve any iterative procedure, and the solution can be obtained once for all by solution of Eq. (14). Furthermore, one only needs to collocate on the boundary to obtain the solution, and interior points are necessary only to improve the interpolation of the forcing function f. Thus, the problem is fully decoupled in this case. The accuracy of the method has been demonstrated for such cases [4].

For the case when f is a function of u, the solution is more involved and involves iterative calculation, since the boundary conditions (needed to find v) are functions of w, whose variation over the domain is unknown. In a variation of the Picard method of iteration implemented by Chen *et al.* [27] for the two-dimensional Dirichlet problem, the v problem is solved by assuming u at the collocation points at the start of the iterations and evaluating the particular solution w at each level of iteration.

One then solves the v problem at the current iteration from the recurrence relation

$$\begin{aligned} \nabla^2 v_{n+1} &= 0 \qquad && \text{over } \Omega \\ v_{n+1} &= \bar{u} - w_n \qquad && \text{over } \Gamma, \end{aligned} \tag{17}$$

where $n+1$ denotes the current iteration and n the previous iteration step.

The particular solution at the previous level of iteration can be evaluated as

$$w_n = \sum_{k=1}^{nt} \psi_k \alpha_{k(n)} \qquad \text{over } \Gamma, \tag{18}$$

where $\alpha_{k(n)}$ in turn is evaluated from Eq. (15), using the f_j values at the nth iteration.

2.4. *Numerical Implementation Using "Matrix of Particular Solutions"*

For linear/mildly non-linear problems, the modified Picard iterative scheme works well. However, the method is very inefficient, and for strongly non-linear problems, the method fails to converge. To improve the convergence, the problem was reformulated in the following manner.

The dependent variable u is now directly expressed as a sum of the homogenous part v and the particular solution w as in Eq. (14). Furthermore, one can now express the values

of α_k as

$$\alpha_k = \sum_{m=1}^{nt} E_{km} f_m \qquad (k = 1, 2, \ldots, nt), \tag{19}$$

where E_{km} represents the elements of the matrix Φ^{-1}, and nt represents the total number of collocation points.

Now one can write the particular solution w given by Eq. (11) as

$$w = \sum_{k=1}^{nt} \psi_k \alpha_k = \sum_{k=1}^{nt} \psi_k \sum_{m=1}^{nt} E_{km} f_m. \tag{20}$$

Changing the order of summation,

$$w = \sum_{m=1}^{nt} \beta_m f_m \qquad \text{with } \beta_m = \sum_{k=1}^{nt} \psi_k E_{km}. \tag{21}$$

Thus, the particular solution can be rewritten in terms of the function values at the nodes rather than in terms of a set of interpolation coefficients. This is a key step in the rapid numerical implementation of the method.

Using the above form of particular solution (Eq. (21)), u and $\frac{\partial u}{\partial n}$ for node i can be written as

$$u_i = a_0 + \sum_{k=1}^{n} a_k G_{ik} + \sum_{m=1}^{nt} \beta_{im} f_m \qquad (i = 1, 2, \ldots, nt) \tag{22}$$

$$\left.\frac{\partial u}{\partial n}\right|_i = \sum_{k=1}^{n} a_k \frac{\partial G_{ik}}{\partial n} + \sum_{m=1}^{nt} \beta'_{im} f_m, \tag{23}$$

where

$$\begin{aligned} \beta'_m &= \sum_{k=1}^{nt} \frac{\partial \psi_k}{\partial n} E_{km} \\ \frac{\partial \psi_k}{\partial n} &= \frac{1}{r_k}[(x - x_k)n_x + (y - y_k)n_y]\frac{\partial \psi_k}{\partial r_k} \qquad \text{in 2-D,} \end{aligned} \tag{23a}$$

where r_k is the distance between (x, y) and (x_k, y_k), and n_x, n_y are components of the outward normal.

One can rewrite Eq. (22) in compact matrix form as

$$\vec{\mathbf{u}} = \mathbf{a}_0 + \tilde{\mathbf{G}}\,\vec{\mathbf{a}} + \tilde{\boldsymbol{\beta}}\,\vec{\mathbf{f}},$$

where $\vec{\mathbf{u}}$ is the vector of concentration values at the nt collocation points, $\vec{\mathbf{a}}$ is the vector of coefficients a_1 through a_n, $\tilde{\mathbf{G}}$ is the matrix of G_{ik}'s, $\tilde{\boldsymbol{\beta}}$ is the matrix of β_{im}'s, and $\vec{\mathbf{f}}$ is the vector of f_i's. A similar vector representation can also be written for Eq. (23) at the collocation points.

The matrix $\boldsymbol{\beta}$, called the *matrix of particular solutions*, offers considerable computational advantage, which will be elucidated in Section 5. The solution is formulated as follows.

The values of u at the nt nodes (both boundary and interior) are assembled using Eq. (22) for a Dirichlet problem. The boundary conditions on $n+1$ boundary nodes are imposed on each equation and one gets a system of nt non-linear algebraic equations for a Dirichlet problem. For a Dirichlet–Neumann (D-N) problem both u and the specified flux $\frac{\partial u}{\partial n}$ at the Neumann boundaries are assembled into the global collocation matrix. In this case, the concentrations at the flux-specified boundaries are additional unknowns in the formulation. If nn is the number of nodes with a Neumann boundary condition, one has to solve for $nt+nn$ variables with as many non-linear algebraic equations in the collocation version of the formulation. When Robin conditions are imposed on part of a domain, one has a convective boundary condition of the form

$$\frac{\partial u_i}{\partial n} = -h(u_i - u_o), \tag{24}$$

where h is the heat/mass transfer coefficient and u_o is u of the surrounding. The equations for the u_i's at the nt collocation points are assembled along with $\frac{\partial u_i}{\partial n} + hu_i$ at the collocation points on the Robin boundaries, resulting in a formulation similar to the one obtained with the Neumann boundary conditions:

$$hu_0 = ha_0 + \sum_{m=1}^{n} a_m \left(hG_{im} + \frac{\partial G_{im}}{\partial n} \right) + h \sum_{k=1}^{nt} \beta_{ik} f_k + \sum_{k=1}^{nt} \beta'_{ik} f_k. \tag{25}$$

Once the set of equations are assembled, they are solved using a quasi-Newton-method-based solver for systems of non-linear algebraic equations, from the standard libraries.

2.5. *Interpolation of f Using Radial Basis Functions*

To approximate the forcing function f one resorts to interpolation using basis functions as in Eq. (8). Various types of basis functions can be used for interpolation. One chooses the basis functions ϕ_k to be radial basis functions, which have been found to be smooth interpolators of multidimensional scattered data in regular and non-regular geometries [4, 26, 28–31]. Commonly used radial basis functions are

- linear $\phi_k = 1 + r_k$;
- thin plate spline $\phi_k = r_k^2 \ln[r_k]$;
- multiquadric $\phi_k = (c^2 + r_k^2)^{1/2}$;

here r_k represents the Euclidean distance of the given point from a fixed point k in the domain. The main advantage of using radial basis functions is that they are independent of the dimensionality of the problem, which lends a significant degree of versatility to the formulation, as discussed in the next section. Once one chooses the radial basis function ϕ_k one has to determine ψ_k, which is evaluated by integrating Eq. (10).

The governing equations for ψ_k are therefore given by

$$\frac{1}{r_k} \frac{\partial}{\partial r_k} \left(r_k \frac{\partial \psi_k}{\partial r_k} \right) = \phi_k \qquad \text{in 2-D;}$$

$$\frac{1}{r_k^2} \frac{\partial}{\partial r_k} \left(r_k^2 \frac{\partial \psi_k}{\partial r_k} \right) = \phi_k \qquad \text{in 3-D.}$$

Expressions for the particular solution for various basis functions are listed in Table 1.

TABLE 1
Expressions for Particular Solutions for Various Radial Basis Functions

Dimension	Radial basis function ϕ_k	Particular solution ψ_k
2-D	$1+r_k$	$\frac{r_k^2}{4}+\frac{r_k^3}{9}$
2-D	$r_k^2\log(r_k)$	$\frac{r_k^4\log(r_k)}{16}-\frac{r_k^4}{32}$
2-D	$r_k^2+r_k^3$	$\frac{r_k^4}{16}+\frac{r_k^5}{25}$
2-D	$(r_k^2+c^2)^{1/2}$	$-\frac{c^3\log\{c\phi_k+c^2\}}{3}+\frac{\{(r_k^2+4c^2)\phi_k\}}{9}$
3-D	$(r_k^2+c^2)^{1/2}$	$\left(\frac{5c^2}{24}+\frac{r_k^2}{12}\right)\phi_k+\frac{c^4[\ln(r_k+\phi_k)-\ln(c)]}{8r_k}$
3-D	$r_k^2+r_k^3$	$\frac{r_k^5}{25}+\frac{r_k^6}{36}$

In our implementation, we have used Hardy's multiquadrics in both two and three dimensions, since it has been shown to have exponential convergence [32].

2.6. *Implementation in Three Dimensions*

A unique feature of the solution methodology is that it is independent of the dimensionality of the problem. To implement the formulation in three dimensions, one only has to replace the G_i functions with the fundamental solution to the three-dimensional potential problem and use the approximate particular solution for the three-dimensional case.

For the method of fundamental solutions,

$$\nabla^2 G = -\delta(r) \qquad \text{where } \nabla^2 = \frac{1}{r^2}\frac{\partial}{\partial r}\left(r^2\frac{\partial}{\partial r}\right), \tag{26}$$

which gives

$$G_i = 1/r_i, \tag{27}$$

where r_i is the distance between the collocation point and the ith source point.

The particular solution ψ_k now satisfies

$$\frac{1}{r_k^2}\frac{\partial}{\partial r_k}\left(r_k^2\frac{\partial \psi_k}{\partial r_k}\right) = \phi_k. \tag{28}$$

The particular solutions for some basis functions in three dimensions are given in Table 1. The remainder of the formulation is exactly the same as before. The use of radial basis functions further enhances this feature, since r_k just has to be modified to

$$r_k = \sqrt{(x-x_k)^2+(y-y_k)^2+(z-z_k)^2}. \tag{29}$$

Thus by just modifying G_i and ψ_k one can use the same numerical scheme, and hence the same code in both two and three dimensions. This is a unique numerical feature of the Trefftz method, which is not shared by any other numerical method.

2.7. *Test Cases*

To test the efficacy of the formulation, two benchmark problems were used, viz. the diffusion–reaction problem and the thermal explosion problem.

i. The diffusion–reaction problem. The diffusion–reaction problem is a classical problem encountered frequently in chemical reaction engineering. The governing differential equation in this case is given by

$$\nabla^2 u = f(u), \tag{30}$$

where $f(u)$ is the forcing function which is generally a function of the dependent variable u. The function f can be of the form $\Phi^2 u^n$, where Φ^2 is called the Thiele parameter and n is the order of the reaction. The parameter Φ^2 represents the ratio of the diffusional resistances to the transport of species to the kinetic resistances on the catalytic surface. As Φ^2 increases, the profiles in the catalyst become steeper near the boundary and for large values, say >25.0, a boundary layer develops at the outer surface of the catalyst. Furthermore, in three-phase systems, part of the catalyst surface can be gas covered or liquid covered, with Dirichlet–Neumann/Robin-type boundary conditions over the perimeter/surface of the catalyst. One thus has a Dirichlet–Neumann singularity at the intersection of the Dirichlet and Neumann boundaries, where the normal gradients are not uniquely defined. The problem is therefore a good test for a numerical method since one can evaluate its ability to resolve the boundary layers and profiles near the singularities, with minimum discretization and computational time. In chemical engineering systems, the problem has to be routinely solved to evaluate the performance of catalyst in terms of the effectiveness factor, which is defined as

$$\eta = \frac{1}{\Omega \Phi^2} \int_{\Gamma} p \, d\Gamma, \tag{31}$$

where Ω, Γ are defined as earlier and p is the normal gradient at the boundary.

ii. The thermal explosion problem. The second problem considered here is the thermal explosion problem. The governing equation to the problem is the Frank–Kamenettski equation,

$$\nabla^2 u = -\delta \exp[u]. \tag{32}$$

This equation is frequently encountered for determination of regimes of safe operation for combustion and other exothermic processes. An important quantity to be determined is the critical value of the parameter δ, δ^*, which represents the point above which no steady-state solution exists, i.e., the system goes into runaway. For various geometries, one can estimate the critical parameter δ^* to ascertain the safe regimes of operation. Since the problem is highly non-linear, it provides a good benchmark for testing numerical schemes. The results obtained using the current formulation were corroborated with those of Chen [27] for the thermal explosion problem with Dirichlet boundary conditions.

2.8. *Source Point Location for the Method of Fundamental Solutions*

As outlined in the literature [4, 33, 34], the source points which are located outside the domain were placed on the perimeter of a circle of a chosen radius so as to achieve convergence. This methodology for locating source points is satisfactory for Dirichlet problems and Dirichlet–Neumann problems with no strong singularities. However, for the cases when

a strong Dirichlet–Neumann singularity exists, a uniform distribution of the source points results in poor convergence or large errors near the singularity. The solutions converged only for a limited number of cases, viz. with low Thiele parameters Φ. To improve the convergence of the scheme we have devised the following heuristic. Here the sources were distributed non-uniformly such that the source points are closer to the Neumann boundaries and further away from the Dirichlet boundaries. This distribution of source points vastly improves the convergence of the method for problems with strong singularities. Such a heuristic can also be used as a starting solution for the source point optimization using least square collocation as outlined in [8], to obtain efficient convergence along with minimal error.

3. RESULTS

The F-Trefftz method was tested for a number of cases in two and three dimensions, and the efficacy of the method will be shown for the benchmark problems discussed earlier. The radial basis function used for interpolation in both 2-D and 3-D was Hardy's multiquadrics [28], for which

$$\phi_k = \left(c^2 + r_k^2\right)^{1/2}.$$

The value of the shift parameter c should be as large as possible for accurate interpolation. However, the convergence of the numerical schemes deteriorates as c increases due to ill-conditioning of the interpolation matrix Φ. The value of c was chosen to be equal to the minimum distance between grid points for each case, using which the scheme converged for all the cases considered. The particular solutions for this case, ψ_k in 2-D and 3-D, are listed in Table 1. The geometries considered in 2-D were a square slab of unit side and a circle of unit radius.

A number of cases were studied to demonstrate the accuracy of the method. In Cases 1 and 2, the results presented are for those cases where the source points were uniformly distributed along the perimeter of a circle for 2-D problems. In Cases 3–5, the results presented are for a non-uniform distribution of sources outside the domain. This configuration was used for problems for which convergence was not obtained using the uniform distribution of source points. Case 6 illustrates the method for Robin conditions. Cases 7 and 8 illustrate the method for three-dimensional problems with uniform and mixed boundary conditions, respectively.

The convergence of the procedure depends on the placement of the source points which are not known a priori. Hence the location of the source points was varied over a range until convergence was obtained. The criterion for convergence was such that the sum of boundary errors was less than 10^{-3}. For all the cases under consideration, the order of convergence for the quasi-Newton method was for the residual to be $O(10^{-4})$.

For comparison purposes, in all the two-dimensional cases, the constant element dual reciprocity boundary element method (DRM) with the same number of nodes as in the method of fundamental solutions was used. DRM has been shown to be an accurate method for the numerical solution of non-linear Poisson problems with boundary singularities [1, 2, 30]. The method of fundamental solutions/F-Trefftz method is referred to as MFS in Tables 2–15 for brevity.

Case 1: Dirichlet boundary conditions, two-dimensional domain. The geometries considered are the unit circle and a square slab of side $= 1.0$. The circle was centered at (0, 0), and 16 boundary nodes and 49 interior nodes were used to discretize the circle.

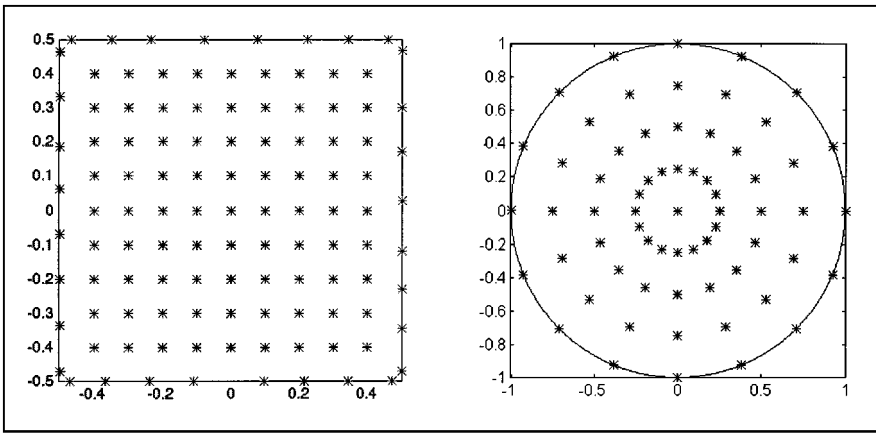

FIG. 2. Collocation point locations for square and unit circle in the base case.

This is illustrated in Fig. 2. Dirichlet boundary conditions were imposed along the perimeter of the circle ($r = 1.0$), which is maintained at $u = 1.0$.

The corners for the square slab are located at (± 0.5, ± 0.5). Thirty-two boundary nodes and 81 interior nodes were used for discretization of the domain. Dirichlet boundary conditions were imposed on all four sides of the square, which are maintained at $u = 1.0$. At the corners of the square, the normal gradients are not defined uniquely. One approach to circumventing this issue is to use double collocation points at the corners. Here the normal gradients are defined corresponding to each side adjoining the corner. Another approach is to have collocation points which are shifted a small distance away from the corners. The latter method of solution was adopted, which is illustrated in Fig. 2. This figure also shows the base case, and the effect of varying levels of discretization is discussed in Section 4.2.

The problems tested were the diffusion–reaction problem and the thermal explosion problem. The test cases for the former are for a first-order and second-order reaction with a Thiele parameter (Φ^2) of 25. For the thermal explosion problem, the critical value of the parameter δ, δ^* was determined by running the code repetitively with small increments in δ, until the program failed to converge, keeping the source radius fixed ($r = 10.0$). This source radius was used to corroborate our results with those of Chen [27].

The results are presented in Tables 2–4, along with a comparison with DRM, from which the accuracy of the method is evident.

Case 2: Dirichlet–Neumann problem, two-dimensional domain. A partially wetted/insulated slab/circle with $u = 1.0$ imposed as the Dirchlet condition and $p = 0$ as the Neumann boundary condition was considered. In both cases the extent of wetting was 50%. As in Case 1, the circle is of unit radius and is centered at the origin. For the circle, the first quadrant $\{\theta = [0, \pi/2]\}$ and the third quadrant $\{\theta = [\pi, 3\pi/2]\}$ are insulated ($p = 0$), while the other two quadrants $\{\theta = [\pi/2, \pi]; \theta = [3\pi/2, 2\pi]\}$ are maintained at $u = 1.0$. The same discretization (16 boundary and 49 interior nodes) was employed as in Case 1 and the situation is illustrated in Fig. 3. The square slab is of side $= 1.0$, with corners located at (± 0.5, ± 0.5) as before. The faces at $x = -0.5$, $x = 0.5$ are maintained at $u = 1.0$, and the faces at $y = -0.5$ and $y = 0.5$ are at insulated ($p = 0$) . As in Case 1, 32 boundary and 81 interior nodes were used to discretize the domain. The collocation points at the corners were placed in the same manner as in Case 1. From Tables 5 and 6, the comparison is good, illustrating the adequacy of the uniform source distribution for this case.

TABLE 2
MFS for First-Order Reaction $f = 25.0u$, Dirichlet Boundary Conditions

Geometry	u (origin) (MFS)	u (origin) (DRM)	Source radius (MFS)
Unit circle	0.0359	0.039	1.9
Square of side = 1.0	0.2572	0.2564	1.5

TABLE 3
MFS for Second-Order Reaction $f = 25.0u^2$, Dirichlet Boundary Conditions

Geometry	u (origin) (MFS)	u (origin) (DRM)	Source radius (MFS)
Unit circle	0.2157	0.2203	1.9
Square of side = 1.0	0.4352	0.4352	2.1

TABLE 4
MFS for Thermal Explosion Problem, $f = -\delta \exp(u)$ Dirichlet Boundary Conditions

Geometry	δ^* (MFS)	δ^* (anal.)	Source radius
Unit circle	2.04	2.0	10.0
Square of side = 1.0	1.71	1.7	10.0

TABLE 5
MFS for a Square Slab of Unit Dimensions (D-N) Conditions

Kinetics	u (origin) (MFS)	u (origin) (DRM)	Source radius
First-order $f = 25u$	0.1729	0.1692	2.3
Second-order $f = 25u^2$	0.3726	0.3689	1.9

TABLE 6
MFS for a Circle of Unit Radius (D-N Conditions)

Kinetics	u (origin) (MFS)	u (origin) (DRM)	Source radius
First-order $f = 25u$	0.02117	0.022	2.1
Second-order $f = 25u^2$	0.1838	0.188	3.0

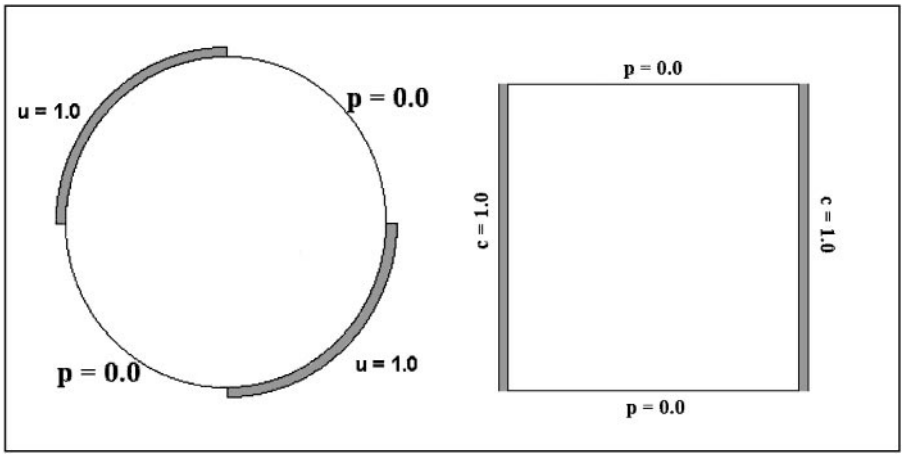

FIG. 3. Configurations for Dirichlet–Neumann problems (Case 2).

Case 3: D-N conditions 50% wetted/insulated, alternate configuration. In this case we consider a square slab of unit side which is wetted/insulated on opposite corners, as shown in Fig. 4. Sixteen nodes were used to discretize the boundary and 64 for the interior of the domain. The corner nodes were placed in the same manner as before. Though this problem has the same fraction of the perimeter insulated, the singularities are much more pronounced than in Case 2, since a D-N junction exists on each side of the square. The fluxes at these junctions are not defined uniquely and the efficacy of a numerical method can be demonstrated by its ability to capture the steep profiles in the vicinity of each

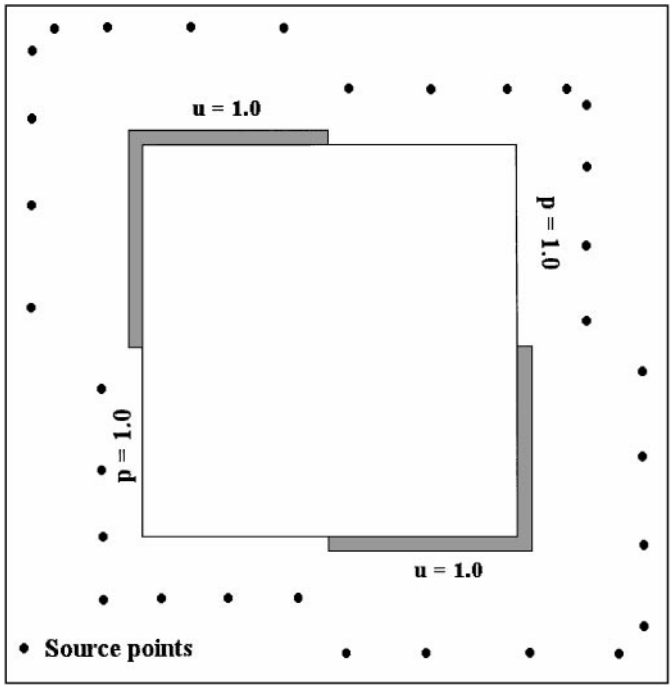

FIG. 4. Configuration and source location for Case 3.

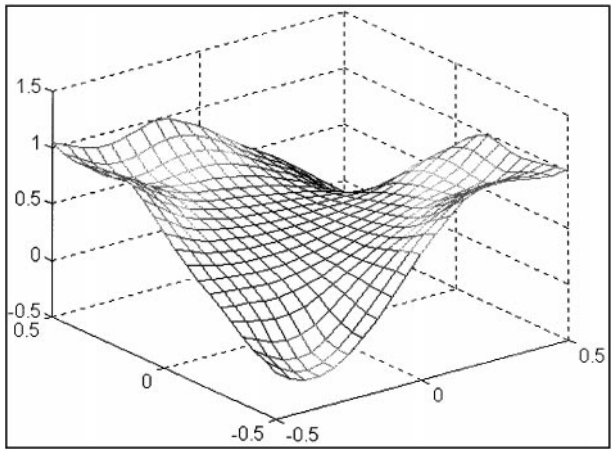

FIG. 5. Concentration profiles for Case 3 ($f = 25u$).

singularity, while preserving the symmetry of the problem. When the sources were located uniformly the method converged only for small values of the Thiele modulus, and the profiles obtained were asymmetric. To improve the convergence the sources were located closer to the Neumann nodes, as illustrated in Fig. 4. By doing so the convergence vastly improved, and the profiles obtained are shown in Fig. 5 for the first-order reaction. Not only does the method now capture the steep gradients in the vicinity of the singularity, but it also preserves the symmetry of the concentration profiles. Table 7 shows the comparison of the MFS solution at the origin with that obtained by the dual reciprocity method, for first- and second-order reactions.

Case 4: Motz diffusion–reaction problem. We consider a slab of side $= 1.0$, where three sides of the square are insulated and half the fourth side is insulated ($p = 0$). The remaining half of one side is maintained at $u = 1.0$. The Laplace problem, with the above boundary conditions, is the classical Motz problem, which is a standard benchmark in numerical analysis. Here we consider the corresponding diffusion–reaction problem. This problem is a particularly stringent test of the efficacy of a numerical scheme owing to the predominance of the Neumann boundaries, the asymmetry of the imposed boundary conditions, and the strong singularity at the junction of the D-N boundary. The slab was discretized using 16 boundary nodes and 64 internal nodes. Hence, Dirichlet boundary conditions were imposed on only two nodes. Here, too, convergence was obtained only with a non-uniform source point distributions, as illustrated in Fig. 6. The concentration profiles are obtained are shown in Fig. 7 for the first-order case. The comparison of the solutions obtained using MFS and DRM are shown in Table 8. The DRM constant element code produced some negative values of fluxes at the boundaries, indicative of the fact that MFS with non-uniform

TABLE 7
MFS for a Slab with Opposite Corners Wetted (Case 3)

Kinetics	u (origin) (MFS)	u (origin) (DRM)	Source radius
First-order $f = 25u$	0.1612	0.1588	Non-uniform
Second-order $f = 25u^2$	0.3608	0.3567	Non-uniform

TABLE 8
MFS for the Motz Diffusion–Reaction Problem

Kinetics	u (origin) (MFS)	u (origin) (DRM)	Source radius
First-order $f = 5u$	0.255	0.251	Non-uniform
Second-order $f = 5u^2$	0.365	0.371	Non-uniform

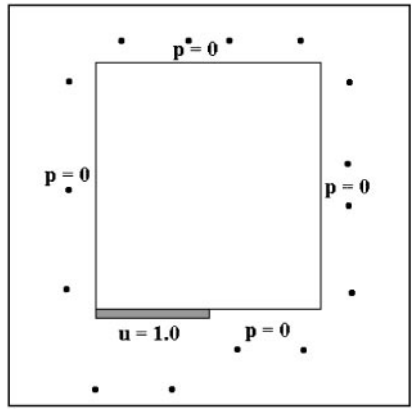

FIG. 6. Configuration and source location for the Motz diffusion–reaction problem.

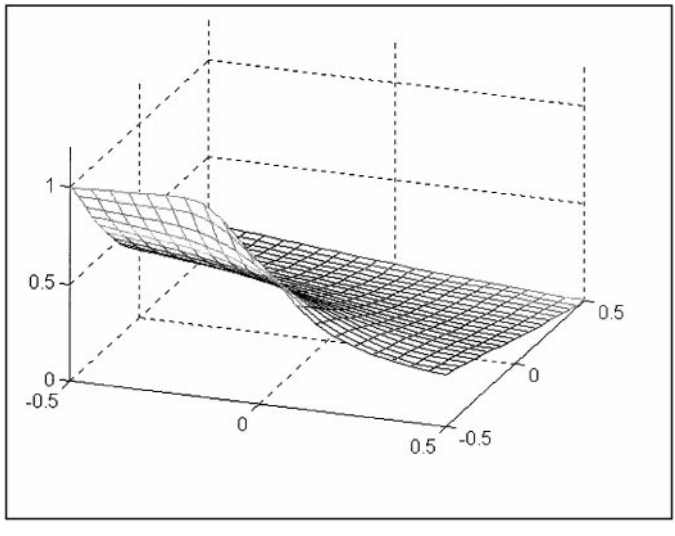

FIG. 7. Concentration profiles for the Motz diffusion–reaction problem ($f = 5u$).

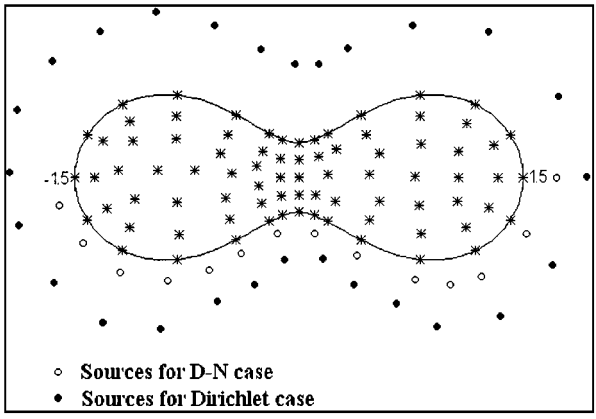

FIG. 8. Discretization and source location for Case 5.

source distribution works better at the low level of discretization. Higher order elements can resolve the steep gradients much better in DRM [2] but at a higher cost of discretization.

Case 5: MFS for the oval of Cassini. To demonstrate the efficacy of the MFS for irregular geometries, we consider the oval of Cassini [4], whose parametric equation is given by

$$\begin{aligned} x &= r(\theta)\cos(\theta) \\ y &= r(\theta)\sin(\theta) \\ r(\theta) &= \sqrt{\cos(2\theta) + \sqrt{1.1 - \sin^2(2\theta)}} \\ 0 &\le \theta < 2\pi. \end{aligned} \tag{33}$$

The geometry and discretization are shown in Fig. 8. The diffusion reaction problem was the test problem with two cases. In one case, Dirichlet boundary conditions, $u = 1.0$, are imposed all along the perimeter. In the other case, Neumann boundary conditions, $p = 0.0$, are imposed along the perimeter for $\pi < \theta < 2\pi$ and $u = 1.0$ is imposed along the rest of the perimeter, as illustrated in Fig. 9. The forcing function f for both cases was $f = 5.0u$.

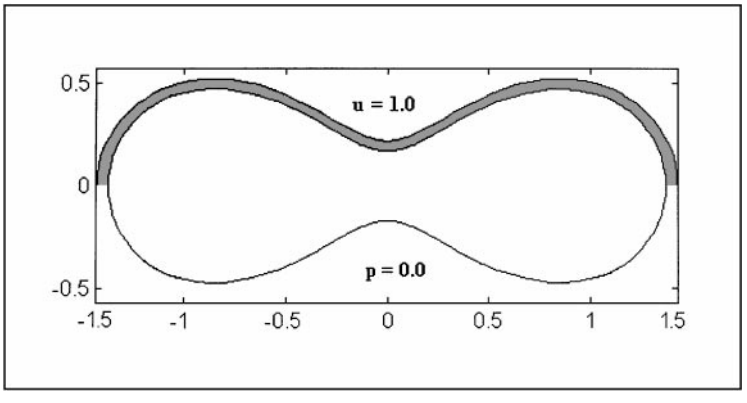

FIG. 9. Dirichlet–Neumann configuration for the oval of Cassini.

TABLE 9
MFS for the Oval of Cassini ($f = 5u$)

Boundary conditions	u (origin) (MFS)	u (origin) (DRM)	Source radius
Dirichlet	0.794	0.786	Non-uniform
Dirichlet–Neumann	0.559	0.573	Non-uniform

The source point location for both cases is shown in Fig. 8. For the D-N problem, half the source points were moved closer to the Neumann boundary. Table 9 shows the comparison of the MFS and DRM solution at the origin.

Case 6: Robin boundary conditions (2-D domain). In this case, we consider a unit circle centered at the origin, as in Case 2. Here, part of the domain is maintained at $u = 1.0$, as in Case 2. However, the remainder is exposed to the surroundings, which is at $u_o = 2.0$. The heat transfer coefficient h is 0.1. The discretization is the same as in Case 2, with 16 boundary nodes and 49 internal nodes. The source points were located uniformly along the perimeter of a circle of radius 1.9. MFS and DRM solutions at the origin are compared in Table 10.

Case 7: Sphere of unit radius (3-D), Dirichlet problem. We consider the three-dimensional Poisson problem. The geometry considered is a sphere centered at the origin of unit radius. The sphere was discretized using 58 boundary nodes (on the surface) and 175 internal nodes. The nodes were located on concentric spheres of decreasing radii. Dirichlet boundary conditions were imposed on the surface of the sphere, with $u = 1.0$ at $r = 1.0$. For comparison, a 1-D boundary element code in spherical coordinates was used. The comparison between the 1-D BEM and the MFS in Table 11 is excellent, and demonstrates the accuracy of the MFS for 3-D problems.

Case 8: Sphere of unit radius (3-D), Dirichlet–Neumann problem. As in Case 7, a sphere of unit radius, centered at the origin, is considered. The discretization is identical to that of Case 7. Dirichlet–Neumann boundary conditions are imposed on the sphere. The left hemisphere is maintained at $u = 1.0$, and the right hemisphere is insulated ($p = 0$), as shown in Fig. 10. For this problem, the solution could not be compared with any case in the literature, and Table 12 gives the concentration values at the origin for first- and second-order reactions. For both Cases 7 and 8, the source points were placed on a sphere outside the domain consideration, and the source radius chosen to obtain convergence. This case illustrates the ability of the method to handle three-dimensional problems with mixed boundary conditions.

TABLE 10
MFS for the Dirichlet–Robin Problem (Case 8)

Kinetics	u (origin) (MFS)	u (origin) (DRM)	Source radius
First-order $f = 25c$	0.0247	0.02309	1.9
Second-order $f = 25c^2$	0.2003	0.1986	1.9

TABLE 11
MFS for a Sphere of Unit Radius, Dirichlet Problem

Kinetics	u (origin) (MFS)	u (origin) (1-D BEM)	Source radius
First-order $f = 25c$	0.0672	0.0674	1.9
Second-order $f = 25c^2$	0.2653	0.2667	2.3

TABLE 12
MFS for a Sphere of Unit Radius (D-N)

Thiele parameter (Φ^2)	u (origin) (MFS)		Source radius
	First-order $f = \Phi^2 u$	Second-order $f = \Phi^2 u^2$	
1.0	0.7204	0.7702	1.9
2.0	0.5632	0.6602	1.9
5.0	0.3335	0.4961	1.9

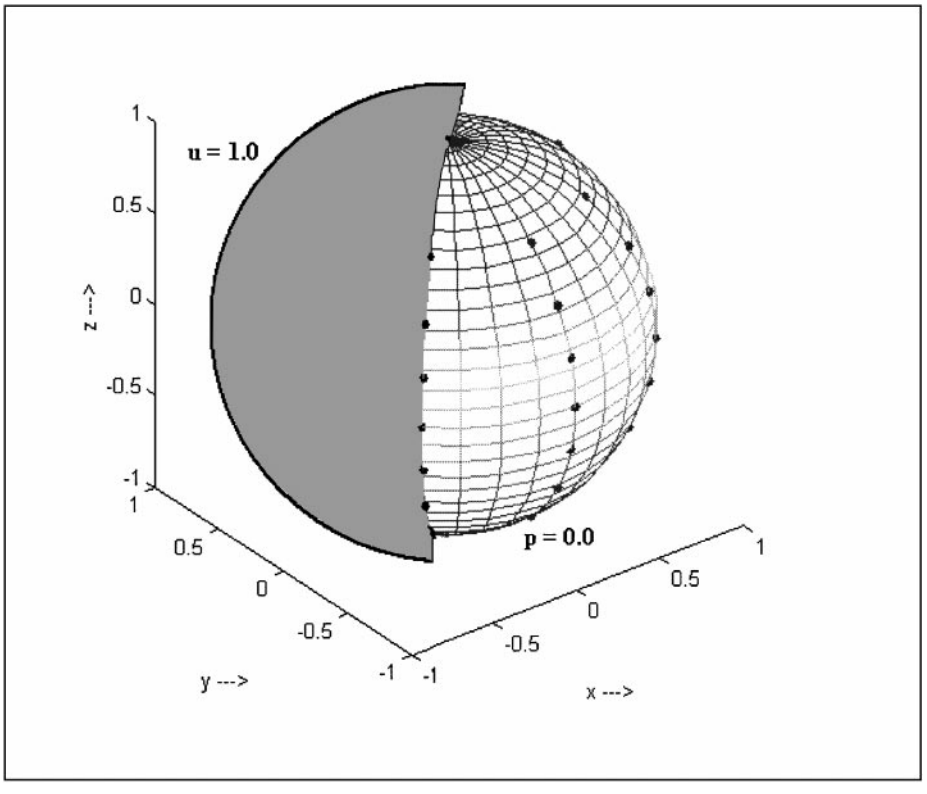

FIG. 10. Configuration for the 3-D Dirichlet–Neumann problem.

TABLE 13
RMS Error over All Nodes for the Base Case

	RMS error (DRM-MFS)	
Case	Square slab	Unit circle
1 ($f = 25u$)	0.0037 (2.3%)	0.01728 (1.9%)
1 ($f = 25u^2$)	0.0032 (2.7%)	0.01687 (2.4%)
2 ($f = 25u$)	0.0414 (5.3%)	0.0801 (4.1%)
2 ($f = 25u^2$)	0.0389 (5.9%)	0.0513 (5.1%)

4. ERROR ANALYSIS AND CONDITIONING OF THE GLOBAL COLLOCATION MATRIX

4.1. *Error Variation with Different Forms of f*

To quantify error of the MFS, the RMS difference between the u values obtained by the MFS and the constant element DRM was calculated over all the nodes. For the 3-D Dirichlet problem, the RMS error was computed by comparison of the 1-D boundary element solution to the problem in spherical coordinates by placing the nodes in the 1-D case at the same radii of the spheres used in the discretization for the MFS.

As one can observe from Tables 13 and 14, the MFS performs relatively well in comparison to DRM for all Dirichlet problems in two and three dimensions. The error over all the nodes was found to be <0.017 in 2-D. However for Dirichlet–Neumann problems the method did show significant errors in comparison to DRM, particularly in the vicinity of the D-N singularity with a uniform source distribution. When the sources were distributed as outlined in Section 2.8, the method performed fairly well in comparison to constant element DRM. For Cases 3 and 4 the DRM constant element required double the number of nodes for satisfactory convergence. Higher order elements in DRM would probably outperform the MFS, but at a higher cost of discretization. Though the magnitude of the error is less for the second-order reaction, one should note that the profiles are steeper for the first-order reaction and hence the error magnitudes are slightly larger.

4.2. *Variation of Error with Discretization Level*

To quantify the error associated with the method with varying amounts of discretization, Cases 1 and 2 for the unit circle were tested with varying amounts of boundary and interior

TABLE 14
RMS Error over All Nodes

Case	Kinetics	RMS error (DRM-MFS)
3	$f = 25u$	9.27×10^{-4} (4.3%)
	$f = 25u^2$	3.72×10^{-3} (4.1%)
4	$f = 5u$	0.028 (3.4%)
	$f = 5u^2$	0.022 (3.2%)
7	$f = 5u$	0.054 (2.3%)
	$f = 5u^2$	0.045 (2.6%)

TABLE 15
RMS Error for Varying Discretization Levels Case 1 and 2 for the Unit Circle ($f = 25u$)

Boundary conditions	No. of boundary nodes	No. of interior nodes	RMS error (DRM-MFS)
Dirichlet	8	25	0.041 (4.4%)
	8	49	0.023 (2.5%)
	16	49	0.0173 (1.9%)
	32	73	6.2×10^{-3} (0.6%)
Dirichlet–Neumann	8	25	0.096 (4.9%)
	8	49	0.087 (4.4%)
	16	49	0.080 (4.1%)
	32	73	0.061 (3.2%)

discretization, as listed in Table 15. One can see that for the Dirichlet problem, the method is sufficiently accurate even for relatively small amounts of discretization. However, for problems with singularities, as in the Dirichlet–Neumann problem of Case 2, the errors are larger. For all cases, the comparison of the RMS error was made with constant element DRM with the largest level of discretization used, viz. 32 boundary and 73 interior nodes. For smaller amounts of discretization, the values of u at the non-collocation points were computed from Eq. (14) for comparison purposes. Since the matrix Φ^{-1} has already been evaluated, the interpolating coefficients α_k can be calculated from the converged solution using Eq. (16).

4.3. *Conditioning of the Global Collocation Matrix*

It has been reported in the literature [4, 18, 20, 27, 35, 36] that the condition numbers of the collocation matrix obtained in the MFS are fairly large. To determine the effect of the conditioning of the global collocation matrix on the convergence of the scheme, the condition number, maximum, and minimum singular values were calculated for some of the test cases. These are listed in Tables 16 and 17. As one can see from the Tables 16 and 17,

TABLE 16
Condition Number, Maximum, and Minimum Singular Values of the Global Collocation Matrix for the Dirichlet and Dirichlet–Neumann Problem in 2-D for the Unit Circle for the Base Case

Test case		Condition number	Maximum singular value	Minimum singular value
Dirichlet	$f = u$	2.28×10^6	32.98	1.44×10^{-5}
	$f = 25u$	3.97×10^6	57.42	1.44×10^{-5}
	$f = u^2$	2.28×10^6	33.11	1.44×10^{-5}
	$f = 25u^2$	3.81×10^6	55.01	1.44×10^{-5}
Dirichlet–Neumann	$f = u$	2.21×10^6	32.99	1.50×10^{-5}
	$f = 25u$	4.61×10^6	68.51	1.50×10^{-5}
	$f = u^2$	2.27×10^6	33.10	1.50×10^{-5}
	$f = 25u^2$	3.21×10^6	47.75	1.50×10^{-5}

TABLE 17
Condition Number, Maximum and Minimum Singular Values of the Global Collocation Matrix Varying Level of Discretization ($f = 25u$)

Boundary conditions	No. of nodes		Condition no.	Maximum singular value	Minimum singular value
	Boundary	Interior			
Dirichlet–Neumann	8	25	1.46×10^6	53.13	3.63×10^{-5}
	8	49	7.13×10^6	119.1	1.54×10^{-5}
	16	49	4.71×10^6	68.51	1.50×10^{-5}
Dirichlet	8	25	2.95×10^5	79.88	2.69×10^{-4}
	8	49	8.25×10^5	90.88	1.10×10^{-4}
	16	49	3.97×10^6	57.42	1.44×10^{-5}

the condition numbers of the global collocation matrix are reasonable when considering the fact that all the computations are performed in double precision. The condition number of the global collocation matrix depends on two factors, viz. the source radius and the Hardy's shift parameter c. An increase in either the source radius or the value of c increases the condition number. This is illustrated in Fig. 11. An increase in source radius improves the solution acuuracy at lower source radii but reaches an asymptote within a certain range, which represents the optimal source radius. Further increasing the source radius increases the condition number without any improvement or even deterioration in the accuracy. For example, for the circle in Case 1, the optimal source radius was around 1.6. A similar argument holds for the shift parameter c. Though the increase in c improves the interpolation accuracy, the condition number of the Φ matrix deteriorates, which in turn results in an

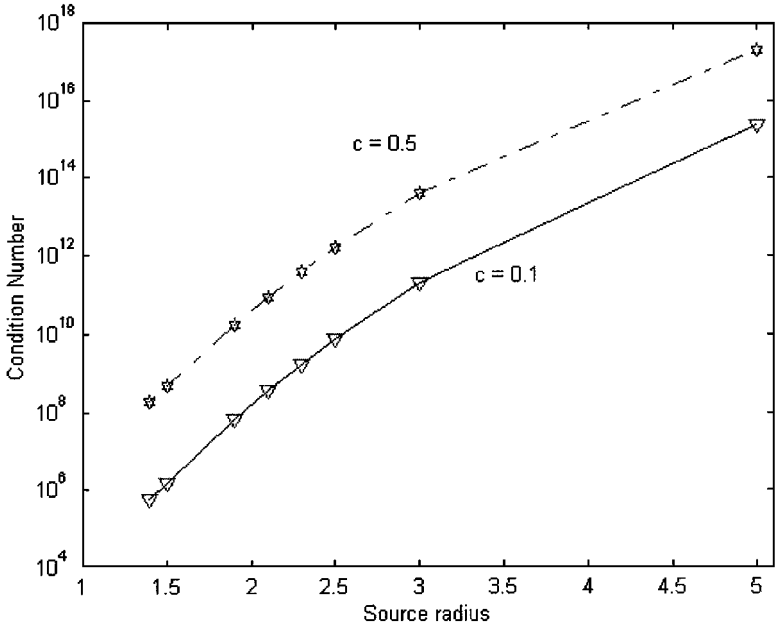

FIG. 11. Variation of condition number with source radius at different values of the shift parameter.

increase in the condition numbers of the global collocation matrix. When $c = 0.5$, the condition numbers are at least three orders of magnitude larger than when $c = 0.1$. As outlined in [37], the shift parameter was chosen to be equal to the distance between the two nearest interpolation nodes. This ensures that the condition numbers are reasonable without sacrificing any accuracy. For cases when a large number of interpolation points are necessary, one can resort to domain decomposition techniques as outlined in the next section for improving the condition numbers.

4.4. *Domain Decomposition for Improving Condition Numbers*

When one has a large number of interpolation points, the use of radial basis functions for interpolation of the forcing function f is not computationally feasible since one has to invert a dense matrix of size $nt \times nt$ where nt is the number of nodes. To reduce the size of the matrix to be inverted one can resort to domain partitioning methods with the appropriate transmission conditions at the interface. To illustrate the use of domain partitioning, the square domain of Case 1 with Dirichlet boundary conditions and $\Phi = 1.0$ was partitioned into two equal domains, as shown in Fig. 12. The transmission conditions at the interface are

$$\begin{aligned} u_1 &= u_2 \qquad \text{on } \Gamma_I \\ \frac{\partial u_1}{\partial n} &= \frac{\partial u_2}{\partial n} \qquad \text{on } \Gamma_I, \end{aligned} \tag{34}$$

where Γ_I is the interface between the two domains.

The advantage of domain decomposition is that when the subdomains have the same geometry, the matrices $\tilde{\boldsymbol{G}}$ and $\tilde{\boldsymbol{\beta}}$ for each subdomain are the same, the only difference being in the boundary conditions imposed. Hence the collocation matrix can be evaluated without any additional matrix calculations for every subdomain. Since the problem is non-linear, an iterative procedure has to be adopted for the interface concentrations/temperature, and

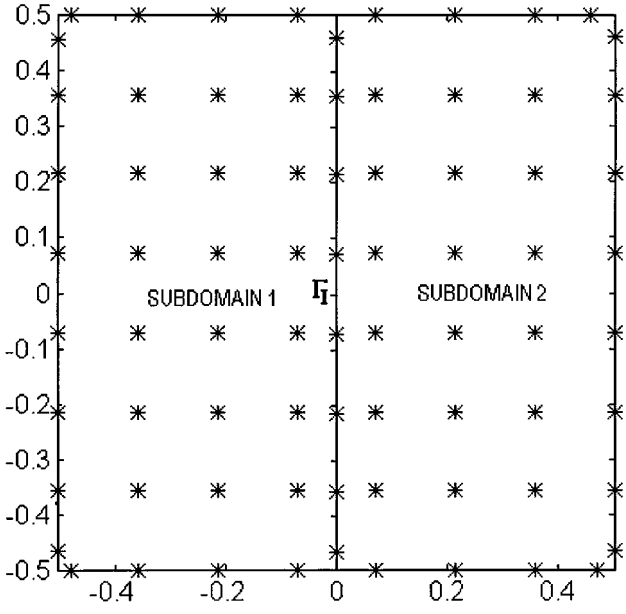

FIG. 12. Domain partitioning for Case 1 ($\Phi = 1.0$).

the alternating Dirichlet–Neumann method [38] is adopted. Here the concentrations/fluxes at the common boundary are arbitrarily specified initially and iterated until convergence is obtained. For this case Dirichlet conditions are specified initially on subdomain 1 and Neumann conditions are specified on subdomain 2. For each iteration, the gradient and the concentration are updated as

$$u^{n+1} = (1-\omega)u^{n-1} + \omega u^{n}, \tag{35}$$

where ω is a relaxation factor. The values of concentration and flux at the interior points are same as the single domain case since both domains are identical. The flux values obtained at the interface are of the order 10^{-4} in comparison to the exact value of 0.0. The advantage of the domain decomposition is the reduction in condition number from 7.8×10^6 to 1.1×10^6 for this particular case. The benefits of domain decomposition will be evident for problems with steep gradients in certain regions, where a large number of nodes can be used along with a small shift parameter. The interpolation in the remainder of the domain can be accomplished using fewer number of interpolation points and a larger value of c.

5. ADVANTAGES AND DRAWBACKS OF THE METHOD

This version of the Trefftz formulation, introducing the concept of a matrix of particular solutions, has considerable computational advantage. The matrix of particular solutions β represents the interaction of the solution at each node with others in the domain and depends only on the location of the collocation points in the domain. The advantage to using the β matrix is that it is independent of the forcing function f and has to be computed only once for a particular geometry and node location. Once the geometry is fixed and one chooses the collocation points, the problem can be solved for various forcing functions and imposed boundary conditions. The matrix of particular solutions is evaluated prior to the iteration procedure, unlike the formulation using Picard's method of iteration, where the coefficients needed to evaluate the particular solution have to be determined at each iteration level. Our formulation using the matrix of particular solutions exhibits superior convergence, corresponding to the quadratic convergence rate of the quasi-Newton method employed to solve the system of equations.

Such a formulation is of immense value in problems in chemical reaction engineering, in two- and three-phase catalytic systems. One notable example is that of catalytic reactions on partially wetted catalyst particles in three-phase reactors. In this context, one needs to evaluate the performance of various catalyst shapes for different kinetic parameters and different wetting configurations. The governing equation is of the same form for all the cases, i.e., the diffusion–reaction equation, with the forcing function f differing for different kinetics, and the boundary conditions varying for different wetting configurations. Since the matrix of particular solutions has to be evaluated only once for a particular geometry, the performance of a particular shape for various kinetic forms can be evaluated at considerable saving of computational cost.

As outlined in Section 2.6, a significant advantage of the formulation is that the solution algorithm is independent of the dimensionality of the problem. One can use the same computer program by simply choosing the appropriate fundamental solution and approximate particular solution in two or three dimensions. This confers a great deal of versatility on the formulation, since one has a method which is both grid free and dimension independent.

A drawback of the method of fundamental solutions is that the radius of source placement for optimal convergence of the scheme is unknown a priori. The method is reported to have exponential convergence within certain radii of source placement [4, 33, 39]. It was observed in our computations that within a certain radius of source placement, as one increases the source radius, convergence was obtained with the same number iterations with improved accuracy, especially for Dirichlet–Neumann problems. Outside this radius of convergence, the number of iterations increased with source radius and the method fails to converge for large source radii. Such behavior can probably be attributed to poor conditioning of the global collocation matrix for large source radius, as discussed in Section 4.3. However, there is no sound theoretical basis by which to determine this radius, so one has to resort to a trial- and-error basis for source placement. For the thermal explosion problem (Section 3, Case 1), it was observed that the convergence of the scheme to find the critical parameter δ^* was dependent to a large extent on the source radius. The scheme failed to converge in some cases for $\delta < \delta^*$, if the source radius was not appropriate.

Another drawback of the formulation is that its convergence is not guaranteed for all problems having singularities, especially those having a large number of flux specified nodes, and in very complex geometries. However, this is a problem encountered by all numerical schemes, and in traditional schemes like finite differences or finite elements, large amounts of discretization help resolve the problem to some extent. Cases 4, 5, and 8 are examples of problems where convergence could be obtained only for low to moderate values of the Thiele parameter Φ. For all these cases, the normal gradients at the junctions of the Dirichlet and Neumann boundaries are not defined uniquely, and the gradient rises steeply in the vicinity of the singularity. For example, the variation in p is of the form $1/r^{0.5}$ near a D-N singularity as for the Motz problem. For larger values of Φ the gradients are extremely steep near the boundaries, and the method fails to capture these gradients accurately. One way to improve the convergence of the method is to use the eigenfunction expansion outlined in [11]. Here basis functions similar to quarterpoint boundary elements are used in the vicinity of the singularity. These functions incorporate the correct variation of the gradient near the singularity and would improve the accuracy of the method for singular problems. The use of orthogonal collocation is another aspect which needs to be investigated [40].

6. CONCLUSIONS AND FUTURE DIRECTIONS

The Trefftz method along with method of particular solutions provides an attractive mesh-free alternative for solving non-linear Poisson problems. The lack of extensive boundary/interior meshing makes the method extremely attractive for two- and three-dimensional problems in non-regular geometries, where the discretization, along with the large amount of bookkeeping involved, can contribute significantly to the total *computational* cost of the exercise in other methods. The proposed new computational scheme using the matrix of particular solutions is shown to possess a number of unique advantages, which makes the method computationally simple and efficient. Further, we have demonstrated the method for various non-linear Poisson problems in two and three dimensions with impressive results. However, in order to make the method more versatile, some refinements are necessary. Some areas which need future consideration are outlined below.

1. *Source point location.* This paper provides a heuristic scheme for locating the source points to obtain superior convergence. As outlined previously, a source point optimization

as outlined in [8] can be implemented to improve the convergence of the MFS, keeping in mind the heuristic for source point location. However, a theoretical analysis of the optimal source location is lacking and needs to be addressed.

2. *Region near singularities.* The method's accuracy and convergence for singular problems are not universal, and a robust method for convergence for a larger class of problems is needed. The convergence of the method can be improved by using special basis functions, in the region of the singularity as proposed earlier. Domain decomposition [41] would provide an attractive means of isolating these singularities to obtain accurate solutions. By doing so one could use mesh refinement in the regions near the singularity without the condition numbers becoming prohibitively large. Least square fitting [42] could also be used to improve the stability of the equations to be solved.

3. *Choice of radial basis functions.* The convergence and accuracy of the method for various basis functions for approximation of the particular of the solution is not shown in this work. The multiquadric was the only basis function used for interpolation. The accuracy of the interpolation of the particular solution can be improved by augmentation of the radial basis functions, viz. multiquadrics [43] and thin plate splines [29], which would reduce the number of the points necessary for interpolation. The location of the discretization knots for interpolation is another aspect which needs to be investigated. Issues relating to knot adaptivity for interpolation of regular and near-singular solutions using radial basis functions have been addressed in [44, 45], and need to be investigated in the context of the Trefftz method.

Use of other basis functions for interpolation of the forcing function is an area currently being investigated. Compactly supported radial basis functions [46] provide a means for making the interpolation matrix Φ sparse, so that iterative solvers can be employed for solution of the resulting equations. For solution of the Poisson equation on a rectangular grid, one can use Fourier series and FFT methods to approximate the particular solution [31]. Some preliminary work in this direction using Chebyshev polynomials has been done with encouraging results [47]. The advantage of using such a method is that the interpolating coefficients α_k in this case can be determined analytically using the orthogonality properties of the basis functions. One can thus obtain the matrix of particular solutions without inverting a dense matrix, thus saving considerable computational labor. Quasi-interpolation [48] is another technique by which one can construct the interpolant without the matrix inversion procedure.

4. *Application to other problems.* This paper has primarily addressed solutions to reaction–diffusion problems. The Trefftz method has been has been used earlier for the solution of potential and Stokes flow problems [24, 49], which involve only boundary collocation, and one could extend the scheme for solution of the Navier–Stokes equations for solutions by approximating the inertial terms using suitable basis functions. This is an area for future research. One could also resort to Lagrangian methods since the grid-free nature of the method would obviate some of the problems of regridding and mesh distortion involved in traditional grid-based Lagrangian methods. The immediate focus of research should be directed toward improvement of the convergence of the scheme and demonstrate its ability to handle a wider variety of problems.

ACKNOWLEDGMENT

The authors acknowledge the National Science Foundation for supporting the work under the auspices of Grant CTS # 9527671.

REFERENCES

1. P. W. Partridge, C. A. Brebbia, and L. C. Wrobel, *The Dual Reciprocity Boundary Element Method* (Computational Mechanics Publications, Boston, 1992).
2. P. A. Ramachandran, *Boundary Element Methods in Transport Phenomena* (Computational Mechanics Publications, Boston, 1993).
3. K. E. Atkinson and D. Chien, Piecewise polynomial collocation for boundary integral equations, *SIAM J. Sci. Statist. Comput.* **76**, 651 (1998).
4. M. A. Golberg and C. S. Chen, *Discrete Projection Methods for Integral Equations* (Computational Mechanics Publications, Southampton, 1996).
5. I. Herrera, Trefftz method, in *Topics in the Boundary Element Method*, edited by C. A. Brebbia (Springer-Verlag, New York, 1984).
6. Y. K. Cheung, W. G. Jin, and O. C. Zienkiewicz, Direct solution procedure for solution of harmonic problems using complete, nonsingular, Trefftz functions, *Commun. Appl. Numer. Methods* **5**, 159 (1989).
7. W. G. Jin, Y. K. Cheung, and O. C. Zienkiewicz, Application of the Trefftz method in plane elasticity problems, *Int. J. Numer. Methods Engrg.* **30**, 1147 (1990).
8. A. Karageorghis and G. Fairweather, The simple layer potential method of fundamental solutions for certain biharmonic problems, *Int. J. Numer. Methods Fluids* **9**, 1221 (1989).
9. A. Karageorghis and G. Fairweather, The method of fundamental solutions for the solution of non-linear plane potential problems, *IMA J. Numer. Anal.* **9**, 231 (1989).
10. A. Karageorghis and G. Fairweather, The method of fundamental solutions for the numerical solution of the biharmonic equation, *J. Comput. Phys.* **69**, 435 (1987).
11. A. Karageorghis, Modified methods of fundamental solutions for harmonic and biharmonic problems with boundary singularities, *Numer. Methods Partial Differential Equations* **8**, 145 (1990).
12. A. V. Khokhlov, Trefftz-like numerical method for linear boundary value problems, *Commun. Numer. Methods Engrg.* **9**, 607 (1993).
13. E. Kita, N. Kamiya, and Y. Ikeda, A new boundary-type scheme for sensitivity analysis using Trefftz formulation, *Finite Elements Anal. Design* **21**, 301 (1996).
14. E. Kita, N. Kamiya, and Y. Ikeda, Application of the Trefftz method to sensitivity analysis of a three-dimensional potential problem, *Mech. Struct. Mach.* **24**, 295 (1996).
15. E. Kita, N. Kamiya, and Y. Ikeda, An application of the Trefftz method to the sensitivity analysis of a two-dimensional potential problem, *Int. J. Numer. Methods in Engrg.* (1996).
16. A. Poullikkas, A. Karageorghis, and G. Georgiou, Method of fundamental solutions for harmonic and biharmonic boundary value problems, *Comput. Mech.* **21**, 416 (1998).
17. C. Y. Chan and C. S. Chen, The method of fundamental solutions for multiple dimensional quenching problems, *Proc. Dynamic Syst. Appl.* **2**, 115 (1995).
18. C. S. Chen, Y. F. Rashed, and M. A. Golberg, A mesh free method for linear diffusion equations, *Numer. Heat Transfer* **33**, 469 (1998).
19. C. S. Chen, *The Method of Fundamental Solutions and the Quasi-Monte Carlo Method for Poisson's Equation. Monte Carlo and Quasi-Monte Carlo Methods in Scientific Computing*, Lecture Notes in Statistics, Vol. 106 (Springer-Verlag, New York, 1995), p. 158.
20. M. A. Golberg and C. S. Chen, The method of fundamental solutions for potential, Helmholtz and diffusion problems, submitted for publication.
21. I. Herrera, *Boundary Methods: An Algebraic Theory*, Applicable Mathematics Series (Pitman, Boston, 1984).
22. M. A. Golberg, The method of fundamental solutions for Poisson's equation, *Engrg. Anal. Boundary Elements* **16**, 205 (1995).
23. M. Katsurada, Charge simulation method using exterior mapping functions, *Jpn. J. Indust. Appl. Math.* **11**, 47 (1994).
24. L. C. Nitsche and H. Brenner, Hydrodynamics of particulate motion in sinusoidal pores via a singularity method, *AICHE J.* **36**, 1403 (1990).
25. M. A. Golberg, The numerical evaluation of particular solutions in the BEM—A review, *Boundary Elements Commun.* **6**, 99 (1995).

26. M. A. Golberg and C. S. Chen, A bibliography on radial basis function approximation, *Boundary Element Commun.* **7**, 155 (1996).
27. C. S. Chen, The method of fundamental solutions for non-linear thermal explosions, *Commun. Numer. Methods Engrg.* **11**, 675 (1995).
28. R. L. Hardy, Multiquadric equations of topography and other irregular surfaces, *J. Geophys. Res.* **176**, 1905 (1971).
29. S. R. Karur and P. A. Ramachandran, Augmented thin plate spline approximation in DRM, *Boundary Element Commun.* **6**, 55 (1995).
30. S. R. Karur and P. A. Ramachandran, Radial basis function approximation in the dual reciprocity method, *Math. Comput. Modeling* **20**, 59 (1994).
31. W. R. Madych, Miscellaneous error bounds for multiquadric and related interpolants, *Comput. Math. Appl.* **24**, 121 (1992).
32. M. A. Golberg, C. S. Chen, and S. R. Karur, Improved multiquadric approximation for partial differential equations, *Engrg. Anal. Boundary Elements* **18**, 9 (1996).
33. M. Katsurada and H. Okamota, The collocation points of the fundamental solution method for the potential problem, *Comput. Math. Appl.* **31**, 123 (1996).
34. T. Kitagawa, Asymptotic stability of the fundamental solution method, *J. Comput. Appl. Math.* **38**, 263 (1991).
35. S. Christiansen and J. Sararen, The conditioning of some numerical methods for first kind integral equations, *J. Comput. Appl. Math.* **67**, 43 (1996).
36. S. Christiansen and P. C. Hansen, The effective condition number applied to error analysis of certain boundary collocation methods, *J. Comput. Appl. Math.* **54**, 15 (1994).
37. D. Funaro, A. Quarteroni, and P. Zanolli, An iterative procedure with interface relaxation for domain decomposition methods, *SIAM J. Numer. Anal.* **25**, 1213 (1988).
38. R. Schaback, Creating surfaces from scattered data using radial basis functions, in *Mathematical Methods for Curves and Surfaces* (Vanderbilt Univ. Press, Nashville, TN, 1995), p. 477.
39. R. S. C. Cheng, *Delta Trigonometric and Spline Methods Using the Single-Layer Potential Representation*, Ph.D. thesis, University of Maryland (1987).
40. S. R. Karur and P. A. Ramachandran, Orthogonal collocation in the boundary element method, *J. Comput. Phys.* **121**, 373 (1995).
41. J. J. Kasab, S. R. Karur, and P. A. Ramachandran, Quasilinear boundary element method for nonlinear Poisson type problems, *Engrg. Anal. Boundary Elements* **15**, 277 (1995).
42. A. P. Zielinski and I. Herrera, Trefftz method: Fitting boundary conditions, *Int. J. Numer. Methods Engrg.* **24**, 871 (1987).
43. E. J. Kansa, Multiquadrics—A scattered data interpolation scheme with applications to computational fluid dynamics, I, *Comput. Math. Appl.* **19**, 127 (1990).
44. E. A. Galperin, Z. X. Pan, and Q. Zheng, Application of global optimization to implicit solution of partial differential equations, *Comput. Math. Appl.* **25**, 103 (1993).
45. Y. C. Hon and X. Z. Mao, An efficient numerical scheme for Burgers equation, *Appl. Math. Comput.* **95**, 37 (1998).
46. M. S. Floater and A. Iske, Multistep scattered data interpolation using compactly supported radial basis functions, *J. Comput. Appl. Math.* **73**, 65 (1996).
47. K. Balakrishnan, R. Sureshkumar, and P. A. Ramachandran, A Chebyshev interpolation based dual reciprocity boundary element method for non-linear reaction-diffusion problems, submitted for publication.
48. R. Pollandt, Solving nonlinear differential equations of mechanics with the boundary element method and radial basis functions, *Int. J. Numer. Methods Engrg.* **40**, 61 (1997).
49. R. L. Johnston and G. Fairweather, The method of fundamental solutions for problems in potential flow, *Appl. Math. Modeling* **8**, 265 (1989).